# Direct measurement of electrical conductance through a self-assembled molecular layer

F. Song[1,2], J. W. Wells[1,3], K. Handrup[1], Z. S. Li[4], S. N. Bao[2], K. Schulte[5†], M. Ahola-Tuomi[6], L. C. Mayor[5], J. C. Swarbrick[5†], E. W. Perkins[1,5], L. Gammelgaard[7] and Ph. Hofmann[1†*]

**The self-assembly of organic molecules on surfaces is a promising approach for the development of nanoelectronic devices[1,2]. Although a variety of strategies have been used to establish stable links between molecules[2-11], little is known about the electrical conductance of these links. Extended electronic states, a prerequisite for good conductance, have been observed for molecules adsorbed on metal surfaces[12-16]. However, direct conductance measurements through a single layer of molecules are only possible if the molecules are adsorbed on a poorly conducting substrate. Here we use a nanoscale four-point probe[17] to measure the conductivity of a self-assembled layer of cobalt phthalocyanine on a silver-terminated silicon surface as a function of thickness. For low thicknesses, the cobalt phthalocyanine molecules lie flat on the substrate, and their main effect is to reduce the conductivity of the substrate. At higher thicknesses, the cobalt phthalocyanine molecules stand up to form stacks and begin to conduct. These results connect the electronic structure and orientation of molecular monolayer and few-layer systems to their transport properties, and should aid in the rational design of future devices.**

Using a good metal as the substrate when studying the electric conductivity of molecular layers on surfaces is problematic because charge will flow through the metal rather than the molecules. A promising substrate for conductance measurements is the silver-terminated silicon surface (Ag/Si(111)–($\sqrt{3} \times \sqrt{3}$); hereafter referred to as Ag/Si), on which the ordered growth of molecular layers can be achieved[5,18–20] and where the substrate consists of a semimetallic surface on a semiconducting bulk. This approach has been chosen in the present paper. Figure 1a shows the measured conductance of the self-assembled layer of cobalt phthalocyanine (CoPc) thickness on the Ag/Si surface. To achieve surface sensitivity, the conductance was measured with a TiW-coated four-point probe with a contact spacing of only 500 nm (refs 17, 21). Also presented are a model of the geometric structure of the film (Fig. 1c) and an image of the type of probe used in the conductance measurements (Fig. 1a, inset).

Two regions of different behaviour can be distinguished. Initially the conductance drops below that of the clean surface (shown in pink). Once the thickness is of the order of one monolayer, the conductance increases again and is eventually even higher than for the clean surface. We interpret this behaviour as the sum of the conductance through two channels: one through the Ag/Si layer and the other as direct conductance through the molecules.

The filled blue circle indicates a situation in which the surface is covered by one layer of flat-lying molecules, defining one monolayer, prepared by evaporating the CoPc molecules on an Ag/Si substrate held at elevated temperature (see preparation details). To facilitate a comparison with the main dataset it is necessary to assign a film thickness to this measurement; here we estimate that one monolayer is equal to 0.3 nm. The conductance for one monolayer prepared in this way agrees well with the main data series for which CoPc was deposited at room temperature, and corresponds to the minimum in the conductance.

There are two factors contributing to the lower conductance when CoPc is adsorbed on Ag/Si. The first is the introduction of disorder, which leads to a higher scattering rate for the carriers. The second, which we propose to be more significant, is related to an electron transfer from the surface to the CoPc molecules. Figure 2a shows X-ray photoelectron spectroscopy data from the cobalt $2p$ core level, for increasing thicknesses of CoPc on Ag/Si. For very small thicknesses, a low binding energy component dominates, whereas at higher thickness, the bulk component dominates. As a comparison, the cobalt $2p$ core level of lithium-doped (that is electron-doped) bulk CoPc is shown in Fig. 2b. Again, two contributions to each peak can be readily identified. For highly doped CoPc, the lower binding energy component dominates whereas for undoped and weakly doped samples, the higher (bulk) component dominates. Thus, by comparing these measurements with those of CoPc on Ag/Si, we propose that the first monolayer of CoPc on Ag/Si is strongly electron-doped.

Also from Fig. 2a, it is clear that the lower binding energy component does not vanish for thicknesses greater than one monolayer. Rather, the higher binding energy component appears in addition. This indicates that the interfacial monolayer of CoPc does not undergo any re-organization. Thus, for thicker films (in which the molecules form in the bulk $\alpha$ geometry), we understand that we still have a strongly electron-doped and flat-lying first monolayer, as shown schematically in Fig. 1c. We later show that the initially confined electron-doping of the first layer is then able to propagate freely through the entire film, leading to increased conductivity.

The photoemission measurements in Fig. 2c show the evolution of the valence band with increasing CoPc deposition. For very thin films (<1 monolayer), there is an increase of intensity close to the Fermi level, but no signature of a peak derived from the highest occupied molecular orbital (HOMO). This, combined with the observed lower conductivity in this thickness range, points towards a strong and localized bonding of the first-layer molecules to the substrate. For thicker films (>1 monolayer), the HOMO begins to appear in the spectra, and from its position and work function measurements (not shown), the
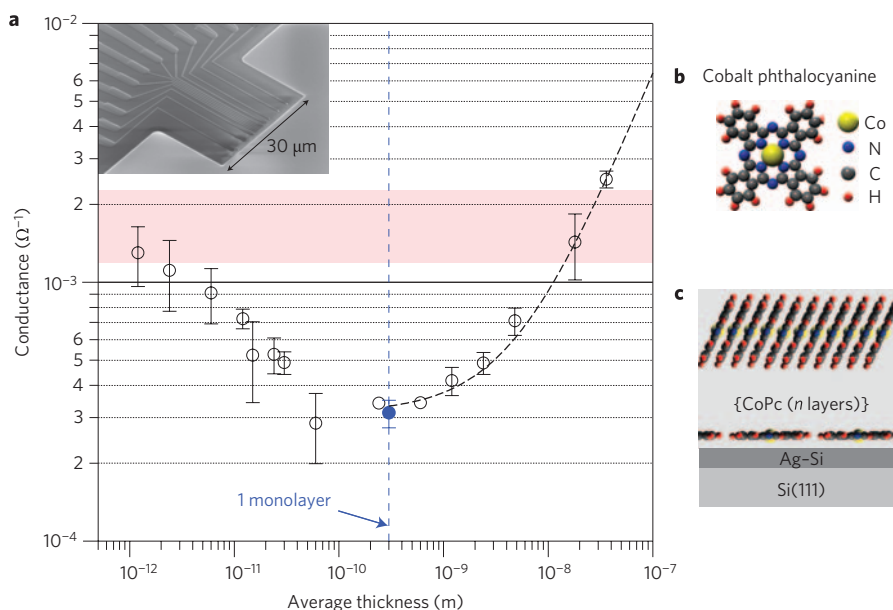
**Figure 1 | Conductance, structure and model of CoPc. a**, Room-temperature conductance of CoPc on ($\sqrt{3} \times \sqrt{3}$)Ag–Si(111) as a function of CoPc average film thickness. Open black circles show data for molecular deposition at room temperature, and the filled blue circle applies to a substrate temperature of 300 °C during deposition, resulting in a film thickness of exactly one monolayer[18], that is, one layer of flat-lying molecules. This thickness is marked by the dashed vertical line. The pink region indicates the conductance of the clean ($\sqrt{3} \times \sqrt{3}$)Ag–Si(111), including experimental uncertainty. The dashed line fitted to the >1 monolayer data points is the result of a conductance model for the system. The inset shows an image of the nanoscale probe used for the measurements[17]. **b**, Structure of a single CoPc molecule. **c**, Model for the geometric structure of CoPc on ($\sqrt{3} \times \sqrt{3}$)Ag–Si(111) based on NEXAFS results (see Supplementary Information). The first monolayer of molecules lies flat on the surface. In a multilayer system the molecular plane encloses an angle of 26° with the surface normal. Note that only the molecules in the first and last layer of a multilayer are shown.

band alignment at the CoPc interface can be estimated (as shown schematically for a thick film in Fig. 2d).

An electron transfer from the surface to the molecular layer can be expected to have a strong influence on the electronic structure and transport properties of the underlying Ag/Si surface termination. The electronic structure of Ag/Si is well known to be semimetallic: it is dominated by a free-electron-like surface state and the bottom of the surface state band is located precisely at the surface Fermi energy[22]. The state is thus unoccupied at zero temperature. At finite temperature it is occupied by thermally excited electrons. Electron-doping of the surface, for example by a small excess silver coverage, shifts the surface Fermi energy upwards, such that the number of free carriers on the surface[22] and the conductivity[23] are strongly enhanced. In the present case the opposite effect is observed; carriers are transferred to the CoPc layer and the surface conductivity drops, as expected.

Interestingly, the minimum conductance is reached when the surface is covered with one layer of flat-lying molecules (the blue filled circle in Fig. 1). This flat-lying structure is observed for thicknesses up to and including one monolayer using scanning tunnelling microscopy[18] and by near-edge X-ray absorption fine structure (NEXAFS) measurements (see Supplementary Information). Hence, an electron-doped but flat-lying layer does not possess a particularly high conductance.

For a higher thickness of CoPc the trend of decreasing conductance is reversed. This is interpreted as conductance through the molecular layer, induced by electron-doping combined with a structural change as more CoPc is deposited on the surface. Our NEXAFS data show that at thicknesses above one monolayer, the molecules start to stand more upright on the surface, forming a layer with stacked π-systems, with an angle of ~26° between the plane of the molecule and the surface normal (Fig. 1; see also Supplementary Information). This stacking is similar to the structure of the α phase of the phthalocyanines[24]. The assumption of

an increased conductance through such a layer is consistent with the observations made for thick films of the CoPc α phase. Although bulk α CoPc is a wide-gap semiconductor, strongly increased conduction can be achieved by n-doping[25] (for a review of the electric properties of similar stacked π-systems see ref. 24).

If we assume that conductance of the thin CoPc film is proportional to its thickness $x$ and given that $x$ is smaller than the spacing between the contacts, we obtain

$$G_{CoPc} = x\pi\sigma_{CoPc}/\ln 2 \qquad (1)$$

where $\sigma_{CoPc}$ is the bulk conductivity of doped CoPc (ref. 26). Because this film is deposited onto the Ag/Si surface, one can assume that the current can pass through both the silver and CoPc layers, and thus the measured conductance is approximated as the sum of the conductance of each layer. The combined conductance ($G_{comb}$) of the two layers is then given by

$$G_{comb} = G_{Ag} + x\pi\sigma_{CoPc}/\ln 2 \qquad (2)$$

where $G_{Ag}$ is the conductivity of the depleted silver monolayer (that is, the conductance of Ag/Si plus one ordered monolayer of CoPc, corresponding to the minimum in the conductance curve). From the data in Fig. 1, $G_{Ag}$ is found to be $3.1 \pm 0.5 \times 10^{-4}\ \Omega^{-1}$, and by fitting the model parameter $\sigma_{CoPc}$ to the data corresponding to $x \geq 0.3$ nm, $\sigma_{CoPc}$ is found to be $1.3 \pm 0.5 \times 10^4\ \Omega^{-1}\ m^{-1}$. The result of the model is depicted by the dashed black line in Fig. 1a and agrees very well with the data.

From the work of others[25] on potassium-doped films of ~20 nm thickness, one can also extract a value for $\sigma_{CoPc}$ in an electron-doped system. This is found to be $\sim 0.3 \times 10^4\ \Omega^{-1}\ m^{-1}$. This is in excellent agreement with our value, given the differences in the experiments and the possible role of defects such as grain boundaries in both our
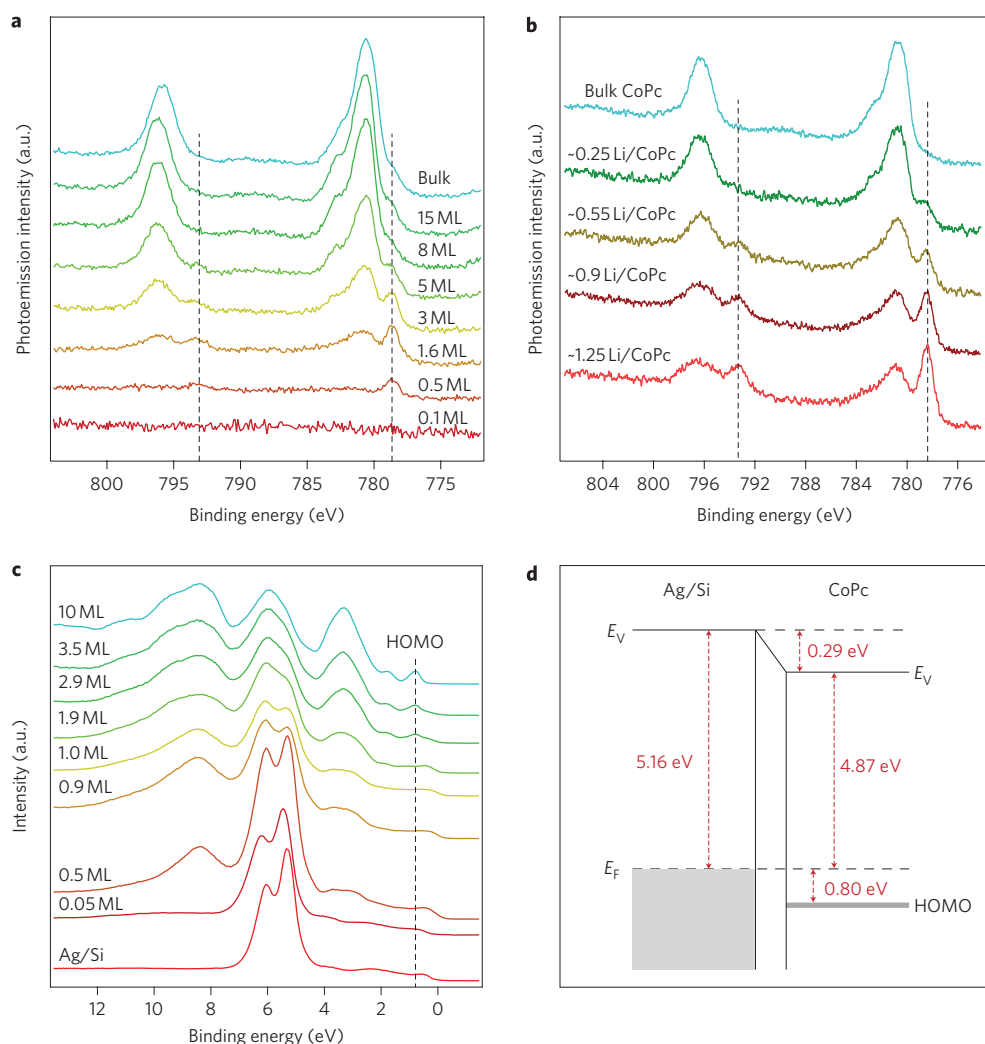
**Figure 2 | Photoemission spectra from different CoPc systems. a**, The cobalt 2*p* core level for CoPc on Ag/Si. The thickness is given in monolayers (ML). Both the bulk component and a smaller surface component (at lower binding energies, marked with dashed lines) are observed. **b**, The cobalt 2*p* core level for lithium-doped bulk CoPc with the number of lithium atoms per CoPc molecule indicated ($h\nu = 920$ eV). Two contributions per peak are present, and the lower binding energy components (marked by dashed lines) are stronger as the lithium doping is increased. **c**, The evolution of the valence band of CoPc on Ag/Si, with the position of the HOMO marked by a dashed vertical line. **d**, Schematic representation of the interface between Ag/Si and bulk CoPc.

work and in ref. 25. Note also that the agreement between our model and the data justifies our assumption of a thickness-independent film conductance. This is consistent with the physical picture of the doping presented above: we assume that charge transfer takes place from the substrate to the molecules in the first layer and this charge is then delocalized throughout the entire film. In thicker films the number of carriers will be smaller, but others have shown that the conductance of electron-doped CoPc is roughly constant over a wide doping range[25].

Note that the space charge layer under the surface does not play any role in the conductance. In the case of clean Ag/Si and for the same bulk doping as in the present study, it has been shown that the space charge layer contribution to the conductance is insignificant[27]. The adsorption of CoPc could, in principle, change the nature of the space charge layer such that it becomes more conductive, but the lower conduction in the initial stages of adsorption cannot be explained by the presence of the space charge layer.

In conclusion, we have shown how the electrical conductivity of self-assembled CoPc evolves as a function of thickness due to the interplay between the geometry and electronic structure of the self-assembled layer and substrate. Once the self-assembled layer reaches a certain thickness, the molecules stack, and conduction occurs mostly through the molecular layer rather than the substrate. For CoPc on Ag/Si, good conductivity is achieved only for films that exhibit π–π stacking between the molecules, and because there is no covalent chemical link between the molecules, the conduction is similar to that in a doped bulk crystal. This is encouraging for strategies that build molecular wires through π–π systems[7] and the general approach outlined here is promising for achieving similar progress for molecules lying on surfaces as for molecules placed between two electrodes[28,29].

**References**
1. Joachim, C., Gimzewski, J. K. & Aviram, A. Electronics using hybrid-molecular and mono-molecular devices. *Nature* **408,** 541–548 (2000).
2. Barth, J. V., Costantini, G. & Kern, K. Engineering atomic and molecular nanostructures at surfaces. *Nature* **437,** 671–679 (2005).
3. Yokoyama, T., Yokoyama, S., Kamikado, T., Okuno, Y. & Mashiko, S. Selective assembly on a surface of supramolecular aggregates with controlled size and shape. *Nature* **413,** 619–621 (2001).
4. Lin, N., Dmitriev, A., Weckesser, J., Barth, J. V. & Kern, K. Real-time single-molecule imaging of the formation and dynamics of coordination compounds. *Angew Chem. Int. Ed.* **41,** 4779–4783 (2002).

5.  Theobald, J. A., Oxtoby, N. S., Phillips, M. A., Champness, N. R. & Beton, P. H. Controlling molecular deposition and layer structure with supramolecular surface assemblies. *Nature* **424,** 1029–1031 (2003).
6.  Barth, J. V., Weckesser, J., Lin, N., Dmitriev, A. & Kern, K. Supramolecular architectures and nanostructures at metal surfaces. *Appl. Phys. A* **76,** 645–652 (2003).
7.  van Hameren, R. *et al*. Macroscopic hierarchical surface patterning of porphyrin trimers via self-assembly and dewetting. *Science* **314,** 1433–1436 (2006).
8.  Grill, L. *et al*. Nano-architectures by covalent assembly of molecular building blocks. *Nature Nanotech.* **2,** 687–691 (2007).
9.  Weigelt, S. *et al*. Covalent interlinking of aldehydes and amines on Au(111) under ultrahigh vacuum conditions. *Angew Chem. Int. Ed.* **46,** 9227–9230 (2007).
10. Yin, P., Choi, H. M. T., Calvert, C. R. & Pierce, N. A. Programming biomolecular self-assembly pathways. *Nature* **451,** 318–323 (2008).
11. Veld, M. I., Iavicoli, P., Haq, S., Amabilino, D. B. & Raval, R. Unique intermolecular reaction of simple porphyrins at a metal surface gives covalent nanostructures. *Chem. Commun.*, 1536–1538 (2008).
12. Netzer, F. P. Determination of structure and orientation of organic molecules on metal surfaces. *Vacuum* **41,** 49–53 (1990).
13. Graen, H. H., Neuber, M., Neumann, M., Odorfer, R. G. & Freund, H. J. Lateral interaction in ordered hydrocarbon overlayers — C–H band dispersion of adsorbed benzene. *Europhys. Lett.* **12,** 173–177 (1990).
14. Yang, W. *et al*. Band structure and Fermi surface of electron-doped $C_{60}$ monolayers. *Science* **300,** 303–307 (2003).
15. Temirov, R., Soubatch, S., Luican, A. & Tautz, F. S. Free-electron-like dispersion in an organic monolayer film on a metal substrate. *Nature* **444,** 350–353 (2006).
16. Yamane, H. *et al*. Electronic structure at highly ordered organic/metal interfaces: Pentacene on Cu(110). *Phys. Rev. B* **76,** 165436 (2007).
17. Gammelgaard, L. *et al*. A complementary metal-oxide-semiconductor compatible monocantilever 12-point probe for conductivity measurements on the nanoscale. *Appl. Phys. Lett.* **93,** 093104 (2008).
18. Upward, M. D., Beton, P. H. & Moriarty, P. Adsorption of cobalt phthalocyanine on Ag terminated Si(111). *Surf. Sci.* **441,** 21–25 (1999).
19. Gustafsson, J. B., Zhang, H. M., Moons, E. & Johansson, L. S. O. Electron spectroscopy studies of PTCDA on Ag/Si(111)–$\sqrt{3} \times \sqrt{3}$. *Phys. Rev. B* **75,** 155413 (2007).
20. Gustafsson, J. B., Zhang, H. M. & Johansson, L. S. O. STM studies of thin PTCDA films on Ag/Si(111)–$\sqrt{3} \times \sqrt{3}$. *Phys. Rev. B* **75,** 155414 (2007).
21. Hofmann, Ph. & Wells, J. W. Surface-sensitive conductance measurements. *J. Phys. Condens. Matter* **21,** 013003 (2009).
22. Crain, J. N., Gallagher, M. C., McChesney, J. L., Bissen, M. & Himpsel, F. J. Doping of a surface band on Si(111)$\sqrt{3} \times \sqrt{3}$–Ag. *Phys. Rev. B* **72,** 045312 (2005).
23. Nakajima, Y., Uchida, G., Nagao, T. & Hasegawa, S. Two-dimensional adatom gas on the Si(111)–($\sqrt{3} \times \sqrt{3}$)–Ag surface detected through changes in electrical conduction. *Phys. Rev. B* **54,** 14134–14138 (1996).
24. Gould, R. D. Structure and electrical conduction properties of phthalocyanine thin films. *Coord. Chem. Rev.* **156,** 237–274 (1996).
25. Craciun, M. F. *et al*. Electronic transport through electron-doped metal phthalocyanine materials. *Adv. Mater.* **18,** 320–324 (2006).
26. Wells, J. W., Kallehauge, J. F. & Hofmann, Ph. Surface-sensitive conductance measurements on clean and stepped semiconductor surfaces: Numerical simulations of four point probe measurements. *Surf. Sci.* **602,** 1742–1749 (2008).
27. Wells, J. W., Kallehauge, J. F. & Hofmann, Ph. Thermal switching of the electrical conductivity of Si(111)($\sqrt{3} \times \sqrt{3}$)Ag due to a surface phase transition. *J. Phys. Condens. Matter* **19,** 176008 (2007).
28. Nitzan, A. & Ratner, M. A. Electron transport in molecular wire junctions. *Science* **300,** 1384–1389 (2003).
29. Wu, S. *et al*. Molecular junctions based on aromatic coupling. *Nature Nanotech.* **3,** 569–574 (2008).

## Acknowledgements

## Author contributions

F.S., J.W.W., S.N.B. and Ph.H. conceived the conductance experiments and F.S., K.H. and J.W.W. designed and performed these experiments and analysed the data. F.S., J.W.W., Z.S.L., K.S., M.A.-T., L.C.M., J.C.S. and E.W.P. performed the photoemission (PES) and NEXAFS experiments. K.S. analysed the NEXAFS and lithium-doping PES, F.S. the thickness-dependent PES. L.G. fabricated the nanoscale four-point probes. Ph.H., J.W.W. and K.S. co-wrote the initial draft of the paper. All authors discussed the results and significantly commented on the manuscript.

## Additional information